Available online at www.sciencedirect.com
SCIENCE DIRECT®
International Journal of Heat and Mass Transfer 47 (2004) 1091–1098
International Journal of HEAT and MASS TRANSFER
www.elsevier.com/locate/ijhmt

A new method for numerical simulation of thermal contact resistance in cylindrical coordinates

Xing Zhang [a,*], Peizhong Cong [b], Seiji Fujiwara [c], Motoo Fujii [a]

[a] Institute for Materials Chemistry and Engineering, Kyushu University, Kasuga, Fukuoka 816-8580, Japan
[b] Interdisciplinary Graduate School of Engineering Sciences, Kyushu University, Kasuga, Fukuoka 816-8580, Japan
[c] Department of Mechanical Engineering, Akashi National College of Technology, Akashi, Hyogo 674-8501, Japan

Received 21 June 2002; received in revised form 10 April 2003

Abstract

In this paper, a random numbers model using an innovative equiperipheral grid in cylindrical coordinates has been proposed to predict the contact spot distribution of two rough surfaces at various loads. The ability of this method to predict the contact spot distribution has been proven through comparison with results using a conventional equiangular grid. Further, a network method using such an equiperipheral grid has been developed in order to solve a three-dimensional heat conduction problem where two cylindrical specimens were connected to each other along the longitudinal direction. A uniform heat flux is given at the bottom surface of specimen I, a uniform temperature is maintained at the top surface of specimen II, and thermal insulation is assumed at the outer radius of the two specimens. The present numerical results have been compared to calculations using conventional equiangular grids and to experimental results obtained for cylindrical brass specimens. The present results are shown to compare much more closely with experimental measurements than previous calculations using conventional numerical models.
© 2003 Elsevier Ltd. All rights reserved.

Keywords: Thermal contact resistance; Solid–solid interface; Random numbers model; Equiperipheral grid; Numerical simulation

1. Introduction

As is well known, thermal contact resistance (TCR) or thermal contact conductance (TCC) ($TCR = TCC^{-1}$) between two solid surfaces plays a significant role in heat transfer in applications such as electronic packaging and nuclear reactors. Many studies [1–10] have been done experimentally and numerically over the past three decades. In our previous papers [11,12], a two-dimensional rough surface model was proposed. Then, numerical simulations on the thermal contact conductance using a network method with conventional equiangular grids in cylindrical coordinates were conducted and the results compared with those measured experimentally for cylindrical brass specimens with flat and wavy rough surfaces. Although the average thermal contact conductance at various contact pressures obtained from the simulations agreed qualitatively with the corresponding experimental results, there were some quantitative differences between them. Further, the contact spot distribution obtained from the simulation showed a higher probability density near the center portion. These differences and unreasonable contact spot distribution are partially attributed to the non-uniform grid area at the conventional equiangular grids in cylindrical coordinates.

In this paper, a new system employing an equiperipheral grid in cylindrical coordinates has been proposed to predict the contact spot distribution for a random numbers roughness model. Further, a network method valid for such an equiperipheral grid has been developed for calculating the cross sectional average thermal contact conductance at the interface of two solid cylinders. The present numerical results have been compared with those obtained from both conventional simulations and previous experiments.

* Corresponding author. Tel./fax: +81-92-583-7638.
E-mail address: xzhang@cm.kyushu-u.ac.jp (X. Zhang).

0017-9310/$ - see front matter © 2003 Elsevier Ltd. All rights reserved.
doi:10.1016/j.ijheatmasstransfer.2003.04.001

Nomenclature

A	scale factor, μm
A_r	real contact area, m^2
D	cross sectional area of test specimen, m^2
f	axial load, N
h_m	thermal contact conductance, $W/m^2\,K$
l	length of specimen, m
L_i	wavelength, m
M	element numbers in radial direction
n	upper limit number of superposed waves
N	element numbers in peripheral direction
p_m	pressure, Pa
q_m	heat flux, W/m^2
r, θ	radius and angle in cylindrical coordinates
r_0	radius of specimen, m
R_a	mean roughness, μm
R_{max1}	maximum roughness of specimen I, μm
R_{max2}	maximum roughness of specimen II, μm
RND	random number
Δr	radial increment, m
Δs	peripheral increment, m
T_c	temperature at the top surface, K
$z(r, \theta)$	surface roughness distribution, μm

Greek symbols

α_i	orientation
λ_a	thermal conductivity of air, W/m K
λ_I, λ_{II}	thermal conductivity of specimens I and II, W/m K
φ_i	initial phase
σ_Y	yield stress, Pa

Subscripts

i	number
r	real
min	minimum
max	maximum

2. Computational method

2.1. Calculation of contact spot distribution

Although various approaches have been proposed, the modeling the contact of rough surfaces is still difficult problem. The difficulty in the development of a theoretical model arises due to the fact that the geometrical configuration of rough surface has a random nature. Based on this consideration, we use a random numbers model where the surface roughness, $z(r, \theta)$, can be expressed as follows.

$$z(r,\theta) = A\sum_{i=1}^{n} \sin\left[\frac{2\pi(r\cos\theta\cos\alpha_i + r\sin\theta\sin\alpha_i)}{L_i} - \varphi_i\right] \tag{1}$$

and

$$A = \frac{R_a}{\frac{1}{D}\int\int\left|\sum_{i=1}^{n}\sin\left[\frac{2\pi(r\cos\theta\cos\alpha_i + r\sin\theta\sin\alpha_i)}{L_i} - \varphi_i\right]\right| r\,\mathrm{d}r\,\mathrm{d}\theta}, \tag{2}$$

where r and θ are the radius and angle in cylindrical coordinates, D and R_a are the cross sectional area of the test specimen and its mean surface roughness, n is the upper limit number of superposed waves used to construct the surface ($n = 64$ in this paper), and L_i, φ_i and α_i are the wavelength, initial phase and orientation at the number i of superposed waves. These parameters can be expressed by the following equations,

$$\begin{aligned} L_i &= (L_{max} - L_{min})\cdot RND_{i,1} + L_{min},\\ \varphi_i &= 2\pi\cdot RND_{i,2},\\ \alpha_i &= 2\pi\cdot RND_{i,3}. \end{aligned} \tag{3}$$

Here $RND_{i,1}$, $RND_{i,2}$ and $RND_{i,3}$ are the random numbers and L_{min} and L_{max} are the minimum and maximum wavelengths respectively.

Based on the above random numbers model, a three-dimensional rough surface for a 20 mm × 20 mm square plate can be constructed as shown in Fig. 1, when the average roughness and minimum and maximum wavelengths are given. Fig. 2 shows a typical two-dimensional surface roughness profile obtained from the present model. The model shows a self-affinity that can be seen by comparing the roughness profiles of the bold curve in Fig. 2(a) and the enlarged profile of the part of bold curve shown in Fig. 2(b).

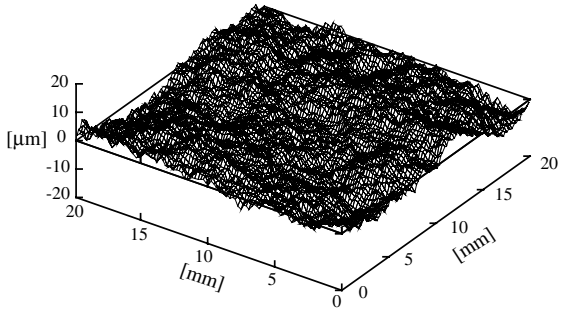

Fig. 1. Simulated 3-D rough surface ($R_a = 2.2$ μm, $L_{min} = 2 \times 10^{-4}$ m, $L_{max} = 2 \times 10^{-2}$ m).

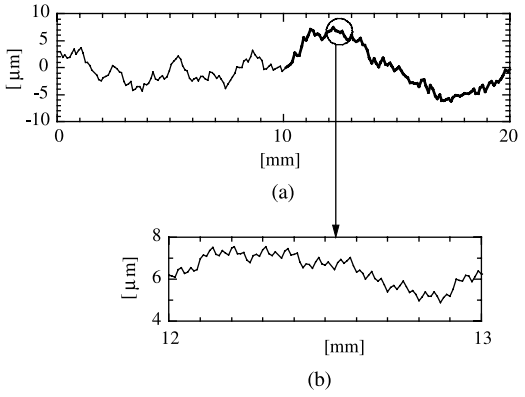

Fig. 2. Self-affinity of surface roughness.

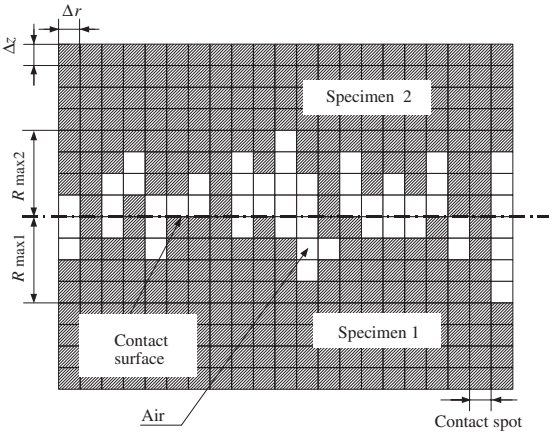

Fig. 4. Contact model.

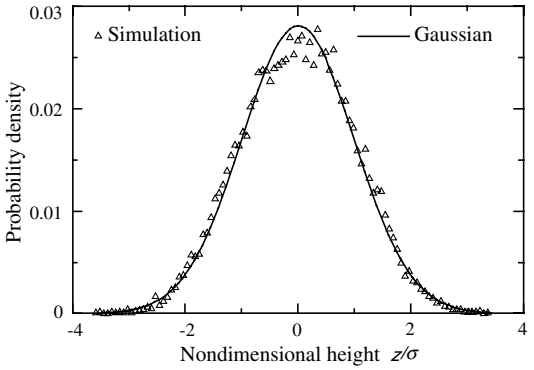

Fig. 3. Height distribution of surface.

Fig. 3 shows a comparison of the probability density function of the present model at mean roughness $R_a = 2.2$ μm with that of a Gaussian distribution. As Johnson [13] pointed out, many real surfaces, notably freshly ground surfaces, exhibit a height distribution close to the 'normal' or Gaussian probability function. The close agreement between the Gaussian distribution and that of the present model validates the use of this model to simulate rough surfaces.

When constructing the surface contact model, we regard the roughness as a solid bar with its bottom surface area equal to respective element area and with height of local roughness. Fig. 4 shows the schematic of the surface contact model, which is an expanded cross sectional view near the contact interface. Lots of voids filled with air (thermal conductivity λ_a) of various thicknesses are distributed randomly over the interface. The deformation of each asperity adopted here is assumed to be fully plastic, and two specimens are pressed together until the following condition [14] is satisfied.

$$f = 3\sigma_Y A_r. \tag{4}$$

Here, f is the axial load, σ_Y is the yield stress (89.2 MPa for brass) and A_r is the total real contact area. It is assumed that the volume of deformed spot in the present method is vanished automatically and does not change the volumes of the neighbor spots.

Fig. 5(a) and (b) show the conventional grid system in cylindrical coordinates and the contact spot distribution obtained by using this grid system. It is noted that the contact spot distribution shows a higher contact probability density near the center portion than the cylinder edge. Such an unreasonable distribution is inherently caused by the conventional grid system. Fig. 6(a) and (b) show the surface roughness profiles along the peripheral direction at $r = 10$ and 20 mm, respectively. The peripheral grid increment at $r = 20$ mm is two times of that at $r = 10$ mm, therefore, the roughness profiles of the latter cannot be expressed with the similar resolution as of the former.

To solve this problem, a new grid system that has equiperipheral increment in whole radial position and also almost the same increments in both the radial and peripheral directions has been proposed as shown in Fig. 7(a). This scheme divided the circle area into three equal, repeatable parts. The total number of elements in the radial (M) and peripheral (N) directions can be expressed by

$$N = 6M + 3. \tag{5}$$

The corresponding peripheral increment (Δs) can be calculated exactly by

$$\Delta s = \pi \Delta r/3. \tag{6}$$

It is noted that the radius of the small circle at the center area equals Δr and M is counted from unity. Based on the above scheme, the contact spot distribution calculated becomes reasonable and independent of the radial position as shown in Fig. 7(b).

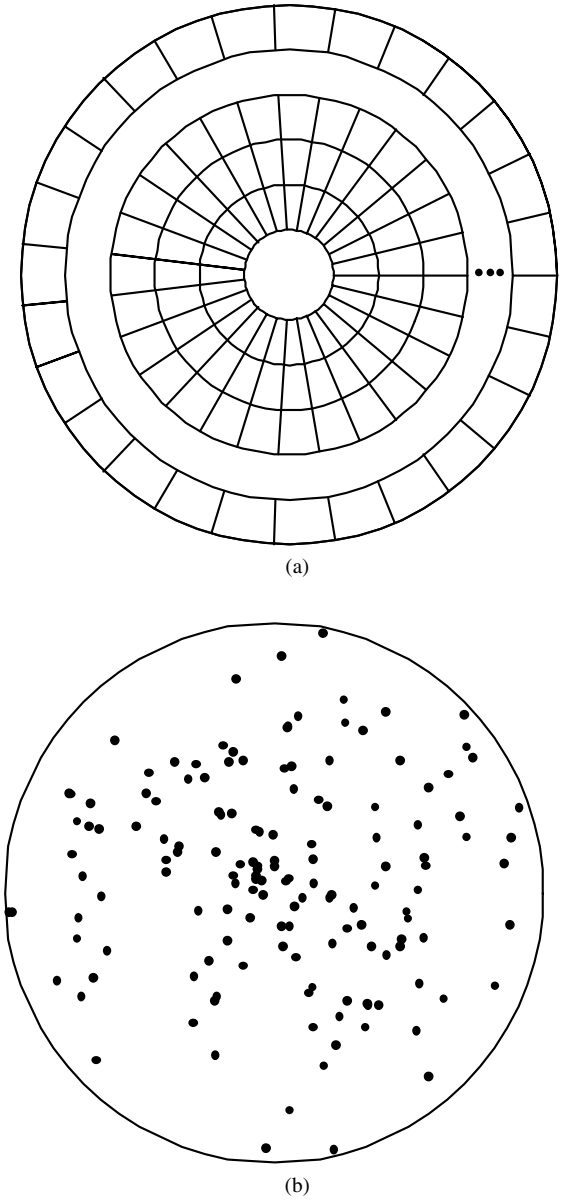

Fig. 5. Conventional equiangular grid system (a) and distribution of contact spots (b).

Fig. 8(a)–(c) show the surface roughness profiles along the peripheral direction at $r = 10$ and 20 mm, and along the radial direction. These profiles show clearly that the model roughness can be expressed with the same resolution in the whole surface area.

2.2. Heat conduction simulations

Fig. 9 shows the physical model and coordinate system for the heat conduction simulations. A pair of

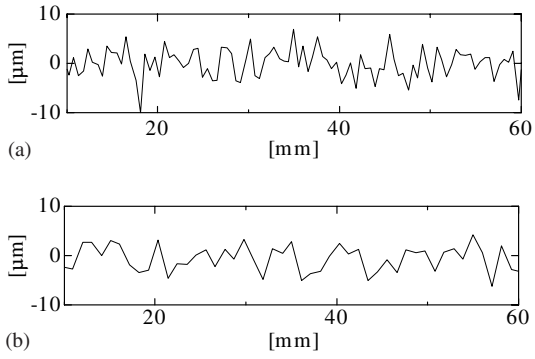

Fig. 6. Surface roughness profiles in peripheral direction: (a) $r = 10$ mm and (b) $r = 20$ mm.

specimens of length l and radius r_0 is pressed together with an axial load f, or an equivalent mean nominal contact pressure p_m. Specimens I and II have the thermal conductivities λ_I and λ_{II} and maximum roughness heights $R_{max\,1}$ and $R_{max\,2}$ respectively. A uniform heat flux is supplied at the bottom surface of the lower specimen ($z = 0$), a uniform temperature is assumed at the top surface of the upper specimen ($z = 2l$), and the side surface of the two specimens ($r = r_0$) is thermally insulated.

As already shown in Fig. 7(b), a reasonable contact spot distribution can be obtained by the equiperipheral grid method. In the present heat conduction simulations, a new network method valid for such an equiperipheral grid is developed to calculate the three-dimensional steady-state heat conduction in a cylindrical coordinate system. Fig. 10 shows the four contact model combinations at the interface region in the z-direction. The harmonic average thermal conductivity is defined respectively. For the combination (a) where the specimens I and II are in direct contact, the harmonic mean thermal conductivity, λ, is estimated by

$$\lambda = \frac{\delta_I + \delta_{II}}{\dfrac{\delta_I}{\lambda_I} + \dfrac{\delta_{II}}{\lambda_{II}}}, \tag{7}$$

where the δ_I and δ_{II} are the lengths between the neighboring nodes and the contact interface and λ_I and λ_{II} are the thermal conductivities of specimens I and II, respectively. For the combination (b) where the specimen I is in direct contact with air, the harmonic mean thermal conductivity, λ, is estimated by

$$\lambda = \frac{\delta_I + \delta_a}{\dfrac{\delta_I}{\lambda_I} + \dfrac{\delta_a}{\lambda_a}}, \tag{8}$$

where δ_a is the length between the neighboring air node and the contact interface and λ_a is the thermal conductivity of air. For the combination (c) where the specimen

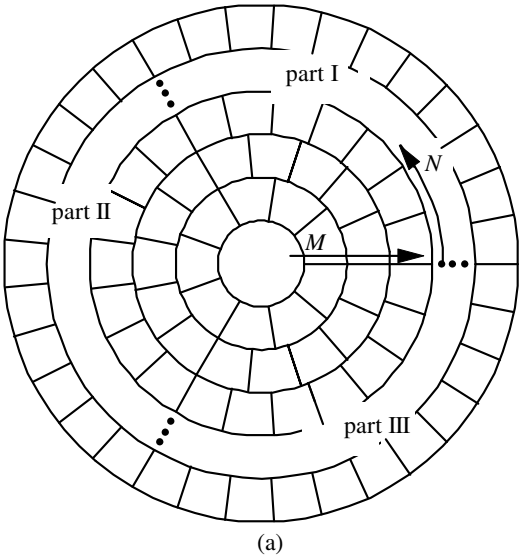

(a)

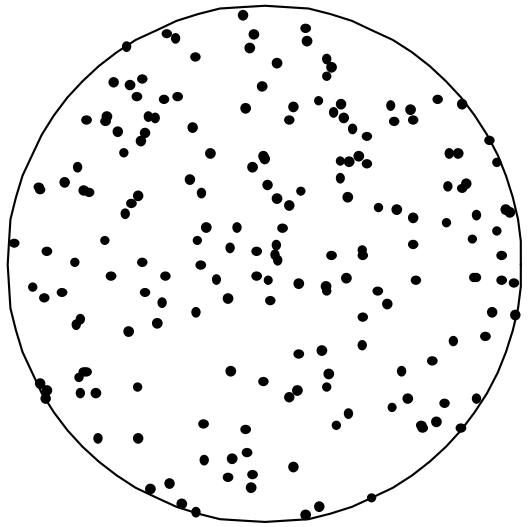

(b)

Fig. 7. Equiperipheral grid system (a) and distribution of contact spots (b).

II is in direct contact with air, the value of λ is calculated by

$$\lambda = \frac{\delta_{II} + \delta_a}{\frac{\delta_{II}}{\lambda_{II}} + \frac{\delta_a}{\lambda_a}}, \tag{9}$$

and finally, for the combination (d) where the specimens I and II are both in contact with air, in this case λ is estimated by

$$\lambda = \frac{\delta_I + \delta_{II} + \delta_a}{\frac{\delta_I}{\lambda_I} + \frac{\delta_{II}}{\lambda_{II}} + \frac{\delta_a}{\lambda_a}}. \tag{10}$$

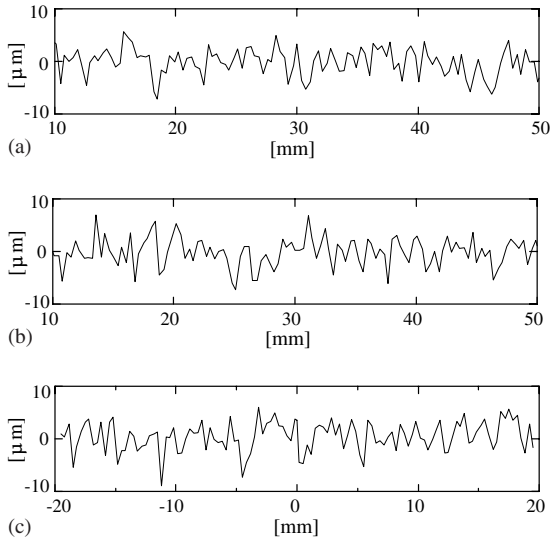

Fig. 8. Roughness profiles in peripheral and radial directions: (a) $r = 10$ mm (in peripheral direction), (b) $r = 20$ mm (in peripheral direction) and (c) r-direction.

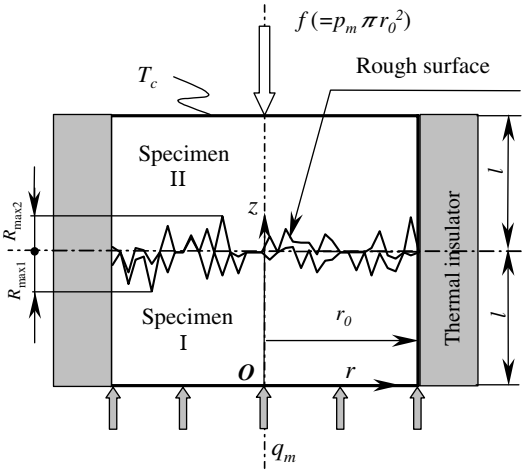

Fig. 9. Physical model for heat conduction simulations.

Fig. 11 shows a typical network system of the equiperipheral grid in the r–θ plane. To calculate the heat flows across the control surfaces perpendicular to the radial direction, the temperatures at the fictitious nodes 1 and 4 adjacent to the control volume 0 can be calculated by interpolation. The temperatures at the peripherally adjacent nodes 2 and 3 can be used directly to calculate the heat flows across the related control surfaces. By using the values of thermal conductivities at nodes 1′, 1″, 4′ and 4″, the thermal conductivities at nodes 1 and 4 are calculated by

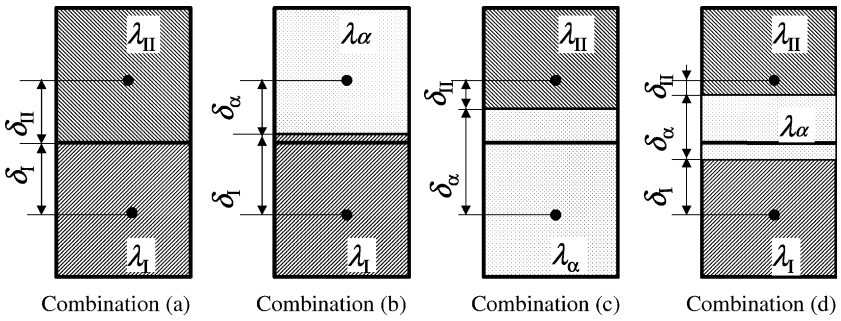

Fig. 10. Contact model combinations in the z-direction.

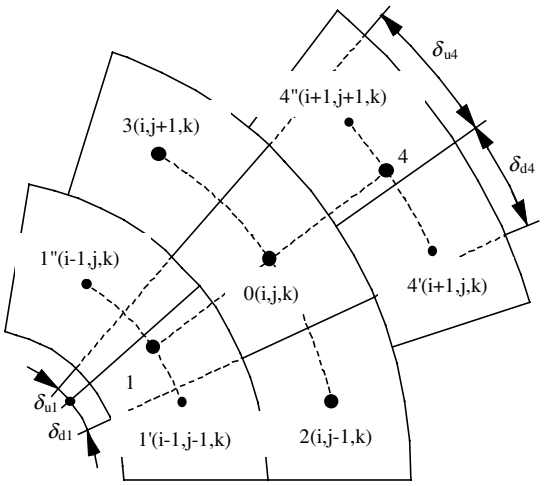

Fig. 11. Equiperipheral grids in the r–θ plane.

$$\lambda_1 = \frac{\delta_{u1} + \delta_{d1}}{\dfrac{\delta_{u1}}{\lambda_{1'}} + \dfrac{\delta_{d1}}{\lambda_{1''}}}, \tag{11}$$

$$\lambda_4 = \frac{\delta_{u4} + \delta_{d4}}{\dfrac{\delta_{u4}}{\lambda_{4'}} + \dfrac{\delta_{d4}}{\lambda_{4''}}}, \tag{12}$$

where δ_{u1}, δ_{d1}, δ_{u4} and δ_{d1} are the peripheral lengths as shown in the figure. Therefore, the harmonic thermal conductivity in the r–θ plane, $\lambda_{i,0}$ can be estimated as follows

$$\lambda_{i,0} = \frac{2}{\dfrac{1}{\lambda_0} + \dfrac{1}{\lambda_i}}, \tag{13}$$

where i represents the node number and changes from 1 to 4. Further, by using the thermal conductivities of nodes neighboring the control volume in the z-direction, λ_5 and λ_6 the remaining two harmonic mean thermal conductivities can be obtained as follows

$$\lambda_{5,0} = \frac{0.5\delta z_k + 0.5\delta z_{k-1}}{\dfrac{0.5\delta z_k}{\lambda_0} + \dfrac{0.5\delta z_{k-1}}{\lambda_5}}, \tag{14}$$

$$\lambda_{6,0} = \frac{0.5\delta z_k + 0.5\delta z_{k+1}}{\dfrac{0.5\delta z_k}{\lambda_0} + \dfrac{0.5\delta z_{k+1}}{\lambda_6}}. \tag{15}$$

A total of nine different combinations for the present equiperipheral grid must be considered, however, the calculation procedure is similar to the above. Once the harmonic mean thermal conductivities and the temperatures at nodes 1 and 4 are obtained, the temperature at node 0 can be calculated with the conventional network method.

To save the computation time, the successive over-relaxation (SOR) method is used. Iteration is terminated when the maximum temperature difference between the successive steps becomes less than 10^{-6}. Fig. 12 shows the effect of grid size on the thermal contact conductance. The thermal contact conductance increases as the number of grids in the radial direction increases, however, the value becomes almost constant when the number exceeds 60. The following results were all obtained using 80 grids in the radial direction.

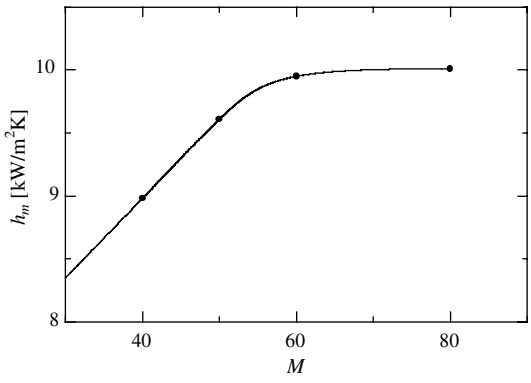

Fig. 12. Relation between M and h_m.

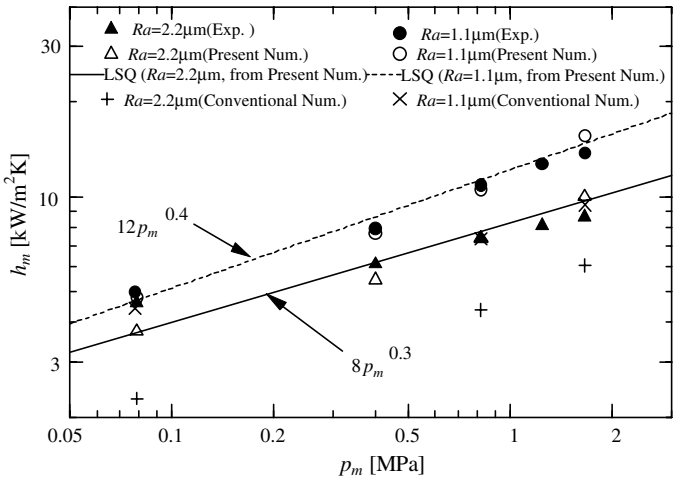

Fig. 13. Relation between p_m and h_m.

3. Results and discussion

As described in our previous paper [11], the thermal contact conductance averaged over the contact interface area is defined by the following equation,

$$h_m = \frac{q_m}{T_{m1} - T_{m2}}. \quad (16)$$

Here, q_m is the mean heat flux and T_{m1} and T_{m2} are the mean contact surface temperatures of the lower and upper specimens, respectively, which are evaluated using an extrapolation method of the temperatures sufficiently away from the interface.

Fig. 13 compares the average thermal contact conductance obtained from the present simulations and previous ones and experiments [11] for the flat rough surfaces. Two cases with roughness $R_a = 1.1$ and 2.2 μm are considered. The large differences are observed between the experimental results and the previous numerical results using the conventional equiangular grid system. While the present numerical results, indicated with open circles and triangles, are greatly improved and agree very well with the experimental measurements. Further, the computational memory and time of the present method are both much less than the previous simulations with the conventional equiangular grid system. This is because the present method can reproduce the fine surface roughness distribution with high and uniform resolution by using fewer total grids than the previous one. Although somewhat complicated methods are needed to construct the network system, the present equiperipheral grid system is found to be very effective to obtain accurately the thermal contact conductance which is independent of grid size.

4. Conclusions

A new method of numerical simulation in cylindrical coordinates has been proposed to calculate the thermal contact conductance at the solid–solid interface. The method is proven to be valid and effective through comparison with experimental results. The main conclusions are as follows.

(1) The surface roughness profile obtained by the random numbers model has the characteristic of self-affinity.
(2) A new grid system that has an equiperipheral increment and a uniform grid area independent of radial position has been proposed. The grid system can reproduce the surface roughness with uniform resolution and predict the reasonable contact spot distribution in cylindrical coordinates.
(3) A network method applicable to the equiperipheral grid system has been developed in order to calculate the thermal contact conductance.
(4) The present numerical results agree very well with those obtained experimentally, compared to those numerical results obtained using the conventional equiangular grid system. Further, the present method requires less computational memory and time.

References

[1] J.A. Greenwood, J.B.P. Williamson, Contact of nominally flat surfaces, Proc. Roy. Soc. (London) A 295 (1966) 300–319.
[2] R.A. Onions, J.F. Archard, The contact of surfaces having a random structure, J. Phys., D.: Appl. Phys. 6 (1973) 289–304.

[3] L.S. Fletcher, Recent developments in contact conductance heat transfer, Trans. ASME, J. Heat Transfer 110 (1988) 1059–1070.
[4] K. Torii, J.I. Yanagihara, Thermal contact resistance in space environment, J. Heat Transfer Soc. Jpn. 28 (110) (1989) 79–99.
[5] A. Majumdar, C.L. Tien, Fractal network model for contact conductance, Trans. ASME, J. Heat Transfer 113 (1991) 516–525.
[6] M.R. Sridhar, M.M. Yovanovich, Review of elastic and plastic contact conductance models: comparison with experiment, J. Thermophys. Heat Transfer 8 (1994) 633–640.
[7] K.-K. Tio, K.C. Toh, Thermal resistance of two solids in contact through a cylindrical joint, Int. J. Heat Mass Transfer 41 (1998) 2013–2024.
[8] W. Yan, K. Komvopoulos, Contact analysis of elastic-plastic fractal surface, J. Appl. Phys. 84 (1998) 3617–3624.
[9] T. Tomimura, T. Kurozumi, X. Zhang, M. Fujii, Estimating the thermal contact conductance of metals by ultrasonic waves, Heat Transfer Jpn. Res. 27 (1998) 130–141.
[10] M.M. Fyrillas, C. Pozrikidis, Conductive heat transport across rough surfaces and interfaces between two conforming media, Int. J. Heat Mass Transfer 44 (2001) 1789–1801.
[11] T. Tomimura, Y. Matsuda, X. Zhang, M. Fujii, Computer simulation of thermal contact conductance based on random numbers, JSME Int. J. 43 (4) (2000) 665–670.
[12] T. Tomimura, Y. Matsuda, X. Zhang, M. Fujii, Two-dimensional modeling of heat transfer between contacting metal surfaces with spherical waviness: estimation of thermal contact conductance based on random numbers surface model, in: B.X. Wang (Ed.), Heat Transfer Science and Technology, Higher Education Press, Beijing, 2000, pp. 137–142.
[13] K.L. Johnson, Contact Mechanics, Cambridge University Press, New York, 1985, pp. 396–452.
[14] F.P. Bowden, D. Tabor, The Friction and Lubrication of Solids, Clarendon Press, Oxford, 1958.